Available online at www.sciencedirect.com

ScienceDirect

Physics Procedia 77 (2015) 21 – 28

Physics Procedia

International Conference on Laser Applications at Accelerators, LA3NET 2015

RF cavity induced sensitivity limitations on Beam Loss Monitors

M. Kastriotou[a,b,c,*], A. Degiovanni[a], F. S. Domingues Sousa[a], E. Effinger[a], E. B. Holzer[a], J. L. Navarro Quirante[a], E. N. del Busto[a,b,c], F. Tecker[a], W. Viganò[a], C. P. Welsch[b,c], B. J. Woolley[a,c]

[a] *CERN, CH-1211, Geneve 23, Switzerland*
[b] *University of Liverpool - Department of Physics, Liverpool L69 7ZE, United Kingdom*
[c] *The Cockcroft Institute, 4 Keckwick Lane, Warrington WA4 4AD, United Kingdom*

Abstract

Due to the secondary showers generated when a particle hits the vacuum chamber, beam losses at an accelerator may be detected via radiation detectors located near the beam line. Several sources of background can limit the sensitivity and reduce the dynamic range of a Beam Loss Monitor (BLM). This document concentrates on potential sources of background generated near high gradient RF cavities due to dark current and voltage breakdowns. An optical fibre has been installed at an experiment of the Compact Linear Collider (CLIC) Test Facility (CTF3), where a dedicated study of the performance of a loaded and unloaded CLIC accelerating structure is undergoing. An analysis of the collected data and a benchmarking simulation are presented to estimate BLM sensitivity limitations. Moreover, the feasibility for the use of BLMs optimised for the diagnostics of RF cavities is discussed.

Peer-review under responsibility of the University of Liverpool

Keywords: Beam Loss Monitors; BLM; dark current; RF breakdown; electron field emission;

1. Introduction

Beam losses refer to fractions of the beam which deviate from the nominal beam orbit and impinge on the accelerator components. Beam Loss Monitors (BLMs) are radiation detectors mounted along the accelerator in order to observe the particle showers generated by beam losses. By monitoring the losses optimal beam transmission, equipment protection from beam induced damages and control of the activation at the surroundings may be achieved. When predefined loss detection levels are reached BLMs are responsible of requesting safe extraction of the beam in circular accelerators, and of preventing the following injection in linacs.

The Compact Linear Collider (CLIC) [1] study proposes a future electron/positron collider where particles will be boosted up to 1.5 TeV by means of normal conducting accelerating structures. To keep the linac in reasonable length, an extremely high accelerating gradient of 100 MV/m will be accomplished via more than 140.000 12 GHz RF cavities. The structures consist of 24 bonded copper cells, one side of which is flat. The other side bears the characteristics of the cell, i.e. four waveguides responsible for the damping of transverse high order modes (HOMs)

* Corresponding author. Tel.: +41-22-76-62425 ; fax: +41-22-76-69593.
E-mail address: maria.kastriotou@cern.ch

Peer-review under responsibility of the University of Liverpool
doi:10.1016/j.phpro.2015.11.005

and four tuning holes for small corrections of the field distribution. Under such high gradient, the surface field of the accelerating structure is estimated to reach 200 MV/m [2]. Imperfections of the cavities enhance field emission of electrons that can be captured by the travelling RF wave and accelerated. This phenomenon is known as dark current [3, 4]. Under high electric field and power flow, locations with enhanced electron field emission may initiate an arching known as RF breakdown. Plasma is formed locally leading to the emission of a current in the order of 100 A with X-rays.

Electrons emitted from the structure may be boosted by the electromagnetic (EM) fields propagating through the cavity to energies that can reach tens of MeV, depending on the distance travelled through the structure. At such energies, electrons impacting on the cavity walls will produce particle showers that can be detected by the BLMs. Therefore, RF cavities will generate signals in neighbouring BLMs even in the absence of beam losses that can be considered as a background and limit the sensitivity of a BLM system

A particle beam propagating through an RF cavity will excite EM fields, a phenomenon known as beam loading [5]. In order to compensate the modification of the cavity fields during beam loading and obtain the nominal accelerating gradient, higher input power needs to be applied to the accelerating structure. At CLIC, the nominal accelerating gradient is achieved via 40 MW (60 MW) input power in the unloaded (loaded) case. To ensure luminosity losses lower than 1%, the CLIC accelerating structures should operate at a maximum breakdown rate (BDR) of $3 \cdot 10^{-7}$ BD/(pulse·m). At the CLIC Test Facility (CTF3) a study on the performance of a CLIC accelerating structure under beam loading is ongoing. The unloaded state can be studied by providing RF power into a structure where no beam is circulating. To examine the effects of high power RF cavities on BLMs, an optical fibre detector has been installed close to the accelerating structure. In the present study, dark current and breakdown events are examined for the unloaded case.

2. Method

2.1. Experimental Setup

At CTF3 the effect of beam-loading on CLIC RF cavities and especially their breakdown rate is being studied. A 24-cell prototype accelerating structure without damping waveguides [6] has been installed in a line branching off the drive beam linac. The structure is connected to a 12 GHz RF source, consisting of a klystron, a pulse compressor and an RF waveguide network. Several RF parameters such as the forward, reflected and transmitted power to the structure are measured [7]. To study the signals induced on the BLMs due to dark current and RF breakdowns, one optical fibre was installed, along the structure and 2.5 cm above it. A large core (900 μm core diameter, 1000 μm cladding diameter, numerical aperture NA = 0.22) Thorlabs pure Silica high-OH multimode fibre [8], 7 m long, was coupled at both ends to a Hamamatsu MultiPixel Photon Counter (MPPC), model S12572-050C [9]. The photodetector was connected to a transimpedance amplifier readout circuit (based on a Texas Instruments THS3061 operational amplifier [10] and a feedback resistor $R_F = 0.5\,k\Omega$). Low noise for the readout was achieved through custom-made low pass filters in the

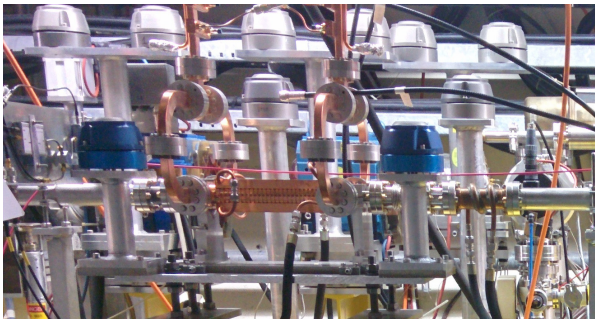

(a) The BLM (red fibre) above the CLIC structure (in the middle)

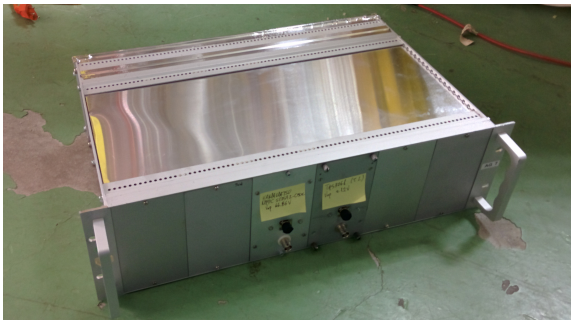

(b) The shielded crate containing the MPPC and the readout electronics

Fig. 1. Installation of the optical fibre BLM at CTF3

voltage supply of the sensor and the amplifier. Shielded modules that contain the photosensor, its readout and the low pass filters were designed to further reduce noise. The modules are mounted in an also shielded crate. The upstream end of the fibre was connected to the above described acquisition system during the period of the present study. The experimental setup is presented in Figure 1(a), while Figure 1(b) shows the crate with the electronics, which is located on the floor, upstream the accelerating structure.

2.2. Methodology

The sensitivity and dynamic range of the system as well as its limitations will be studied in this document in terms of the total charge Q measured by the MPPC sensor. This can be calculated as:

$$Q = \frac{1}{R_L}\int_{t_0}^{t_1}(V_{meas} - V_{off})dt \tag{1}$$

where $R_L = 50\,\Omega$ is the load used at the signal output, V_{meas} the measured pulse amplitude and (t_0, t_1) define the integration interval. The signal offset V_{off} was calculated as the mean value of the first 50 samples and was computed for each pulse independently. The integration window was set to 240 ns for the case of dark current, in order to include the full length of the pulse. For the breakdown cases a longer window of $1.6\,\mu$s was selected, to observe the development of the breakdown. To study the evolution of the BLM signal compared to the input power, the maximum of the forward power to the accelerating structure was recorded.

The number of Cherenkov photons detected by the MPPC can be estimated from the readout circuit design as:

$$N_{ph} = \frac{2 \times R_L}{R_F \times G \times q_e} \times Q \tag{2}$$

where N_{ph} is the number of detected photons, $R_F = 0.5\,k\Omega$ the feedback resistor of the transimpedance amplifier circuit, $G = 1.25 \times 10^6$ the MPPC gain and $q_e = 1.6 \times 10^{-19}\,C$ the electron charge.

In an optical fibre BLM, high energy shower electrons crossing the core produce Cherenkov photons, which propagate through the fibre and are detected by the photodetector. In the case of electrons, the minimum energy to generate Cherenkov light is approximately 200 keV. The number of Cherenkov photons generated in an optical fibre and detected by the photodetector per electron crossing the fibre [12] can be calculated as:

$$\frac{d^2N_{ph}}{d\lambda da} \approx 2\pi\alpha z^2 L \sin^2\theta_C \cdot P_{e,n} \cdot \frac{10^{-\frac{0.83\cdot L_{fib}[km]}{10\cdot\lambda^4[\mu m]}}}{\lambda^2} \cdot \eta_{PDE}(\lambda) \tag{3}$$

where α is the fine structure constant, $z \cdot e$ the charge of the particle crossing the fibre, L_{fib} the length of the fibre travelled by the photons and $\eta_{PDE}(\lambda)$ the photon detection efficiency of the MPPC. The characteristic emission angle of the Cherenkov light θ_C has been estimated from $\cos\theta_C = \frac{1}{\beta\cdot n_{co}}$, where $\beta = v/c$ is the relativistic velocity of electrons and n_{co} is the refractive index of the core of the fibre. The electron trajectory length through the fibre core is calculated as $L = \frac{2\sqrt{R^2-b^2}}{\sin a}$, where a is the angle between the electron trajectory and the longitudinal axis of the optical fibre, b is the closest distance of the particle trajectory to the fibre axis and R the fibre core radius. The term

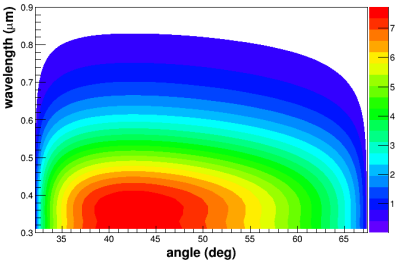

Fig. 2. Double differential number of photons detected by the MPPC per electron crossing an optical fibre, as calculated from Equation 3

$10^{-\frac{0.83 \cdot L_{fib}[km]}{10 \cdot \lambda^4[\mu m]}}$ is related to the attenuation of light in the fibre after covering distance L_{fib} and contains the exponential $1/\lambda^4$ term characteristic of Rayleigh scattering. The $1/\lambda^2$ dependency raises from the Cherenkov light emission spectrum. Finally, the generated Cherenkov photons must be trapped in the optical fibre, propagate to its end face and exit within the nominal acceptance cone. The latter defines the angles under which a ray of light hitting the core of the fibre will be trapped and propagated to its end face. The described probability is given by $P_{e,n}$:

$$P_{e,n} = \frac{1}{\pi} \arccos \frac{\beta \sqrt{n_{co}^2 - NA} - \cos a}{\sin a \sqrt{\beta^2 n_{co}^2 - 1}} \tag{4}$$

where NA is the numerical aperture of the fibre.

The number of electrons necessary to generate a given BLM signal was estimated via Equation 3. The calculations performed were approximate, and only electrons with relativistic $\beta = 1$ are taken into consideration. The numerical aperture of the fibre was $NA = 0.22$ and $n_{co} = 1.47$ for quartz. Since the central part of the fibre is mounted close to the structure, it was assumed that all electrons cross the fibre at its longitudinal centre, hence that the photons propagate for $L_{fib} = 3.5\,m$ until they are detected. For the electron trajectory L, the mean value of the term $2\sqrt{R^2 - b^2}$ which equals to $\frac{\pi R}{2}$ was considered. The double differential detected photon yield $\frac{d^2 N_{ph}}{d\lambda da}$ for electrons crossing the fibre and with the above parameters is shown in Figure 2. To estimate the number of photons detected per charged particle crossing the fibre, the latter was integrated over all optical wavelengths (200 nm − 900 nm) and trajectory angles (0° − 90°).

3. Results

Five different data-taking periods were selected for this study. The RF pulse length was approximately 200 ns. The periods analysed and the respective input powers, numbers of RF pulses and breakdown data are summarised in Table 1. The statistics for the RF breakdown events are very low compared to the thousands of normal RF pulses. In Figure 3(a) a dark current induced signal is observed over the 10 mV peak to peak noise. The horizontal axis corresponds to the sample number. For the 250 MHz sampling rate of acquisition, one sample is acquired every 4 ns. The width of this signal is consistent with the 200 ns RF pulse length. Figure 3(b) shows a large peak generated during an RF breakdown. The two precursor peaks are generated by the dark current during the two previous RF pulses.

The history plot of the measured peak input power in the RF cavity and the corresponding integrated charge from the BLM for non-breakdown pulses is presented in Figure 4(a). A correlation between the input power and the integrated charge of the BLM is evident. The effect is more distinct when representing the measured charge Q versus the peak input power as shown in Figure 4(b). The small points correspond to the BLM charge and input power for each pulse, whereas the different colors refer to the different data-taking periods. For each period the statistical mean of the charge and the input power were calculated and are included in the figure as black diamond points. It can be observed that the raise of input power leads to a larger BLM signal in absolute value. This can be explained by the

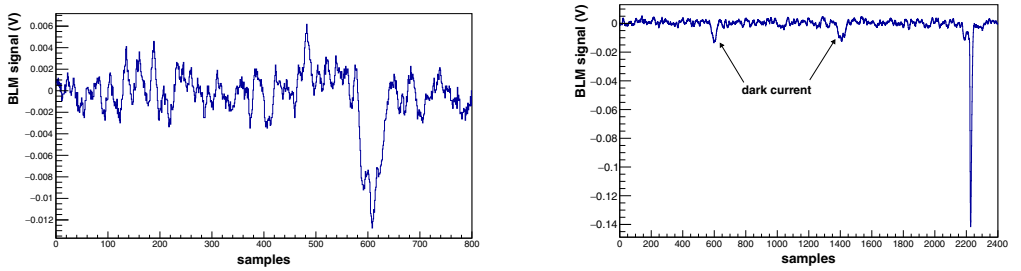

(a) Electron field emission (b) RF breakdown

Fig. 3. Typical BLM signal recorded during unloaded operation

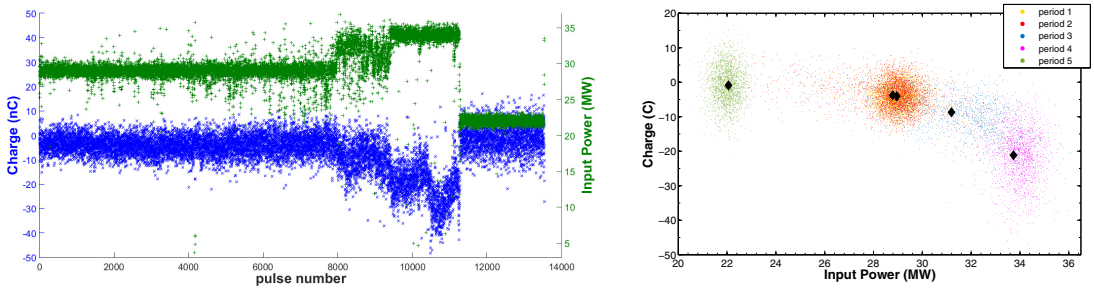

(a) History of peak input power and corresponding BLM integrated charge

(b) BLM integrated charge versus peak input power for different measurement periods

Fig. 4. History plot (left) and correlation plot (right) of BLM integrated charge and structure peak input power

fact that the accelerating gradient of a cavity depends on the input power. Hence, the higher the input power, the higher the energy of the primary particles impinging on the structure, and the more dense the particle shower that will be generated. The same process and calculation of mean values was followed for the case of RF breakdowns during unloaded operation. In this case, the low statistics result in high uncertainty of the measurements.

Table 1. Time period, input power and statistics of the analysed data

Period	Dates	Input Power (*MW*)	non-breakdown pulses	RF breakdown pulses
1	06/10/2014 - 09/10/2014	29.0	4178	47
2	16/10/2014 - 20/10/2014	29.0	3697	65
3	20/10/2014 - 27/10/2014	32.5	1539	51
4	05/11/2014 - 07/11/2014	33.0 to 35.0	1187	218
5	10/11/2014 - 13/11/2014	22.0	2280	3

Figures 5(a) and 5(b) represent the number of electrons crossing the fibre (and detected photons) estimated from the mean integrated charge of each period as described in Section 2.2, as observed during the electron field emission and RF breakdown cases. An exponential behaviour is observed in both cases, which fits well to the function:

$$N(x) = exp(p0 + p1 \cdot x) + p2 \tag{5}$$

where N(x) is the number of detected photons and $p0$, $p1$, $p2$ are the free parameters of the function. The best encountered fit is represented in the figures as a blue line. Extrapolating for the 40 MW nominal power of the unloaded

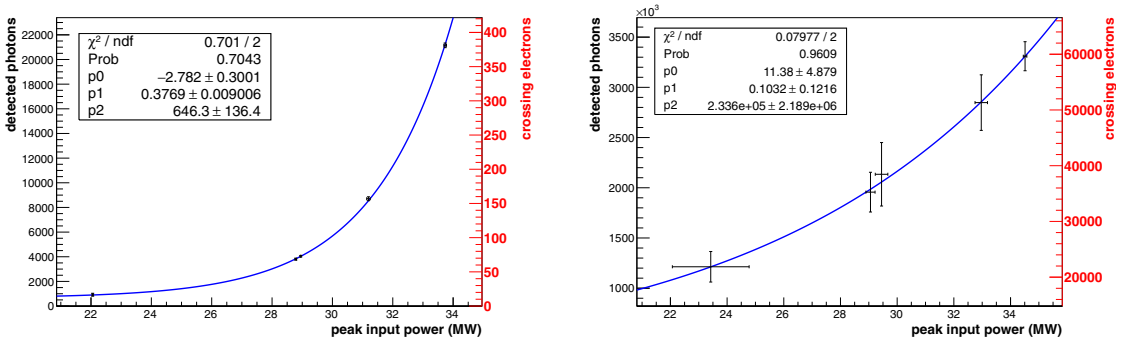

(a) Electron field emission

(b) RF breakdown

Fig. 5. Detected photons and estimation of the number of electrons with $\beta = 1$ that will give the respective signal when crossing the BLM

CLIC accelerating structures and the 60 MW of the loaded, the BLM background induced from field emitted electrons can be estimated and it is described in Table 1. The values calculated are particularly high, reaching for electron field emission 220 nC of BLM charge at 40 MW and 410 μC at 60 MW. This rapid increase of the signal with input power is in good agreement with the increase of field emitted electron current described by the well known Fowler-Nordheim equation [13]. Such large signals can cause a significant limitation in the sensitivity and therefore reduce the dynamic range of the detectors. The same extrapolations in the case of RF breakdown give a charge of 5.67 μC at 40 MW and 43 μC at 60 MW, however due to the lack of statistics and the high uncertainty in the free parameters of the fit ($p0$, $p1$, $p2$), conclusions on the expected background cannot be drawn.

Table 2. Extrapolation of expected dark current signals on BLM at nominal beam power expressed as number of detected photons, number of crossing electrons and integrated charge

	40 MW	60 MW
photons	2.19×10^{5}	4.10×10^{8}
electrons	3.95×10^{3}	7.39×10^{6}
charge (C)	2.19×10^{-7}	4.10×10^{-4}

4. Simulation

A Monte Carlo simulation of electrons impacting onto a CLIC accelerating structure was performed in FLUKA [14, 15] for benchmarking the experimental results. The main target was to examine if field emitted electrons accelerated by the RF cavity can gain sufficient energy to escape through the cavity cells and generate Cherenkov light in the optical fibre. Figure 6(a) presents the simplified geometry, consisting of 24 copper discs of 3.7 cm radius, 0.98 cm thickness and an iris radius of 0.375 cm, which is the average iris radius of the CLIC structure cells. Contradicting the experimental setup, the simulated structure has damping waveguides [16]. The tuning holes were added to each cell. An optical fibre with the same characteristics (900 μm diameter quartz cylinder) and position as the one tested at CTF3 (2.5 cm above the structure) was implemented. The total length of the simulated fibre was 43.12 cm, and it exceeded each side of the structure by 9.8 cm.

Considering an accelerating gradient of 100 MV/m and an RF structure length of approximately 24 cm, interactions of particles impinging on the iris of the twentieth cell of the structure with different energies were simulated. Cell 20 was chosen as an interaction location, because being one of the last discs of the structure, electrons at that point have gained high energies. The interaction point was selected to be the top of the iris and have the minimum distance from the optical fibre. Due to the accelerating gradient it can be considered that an electron gains 1 MeV/cm while travelling

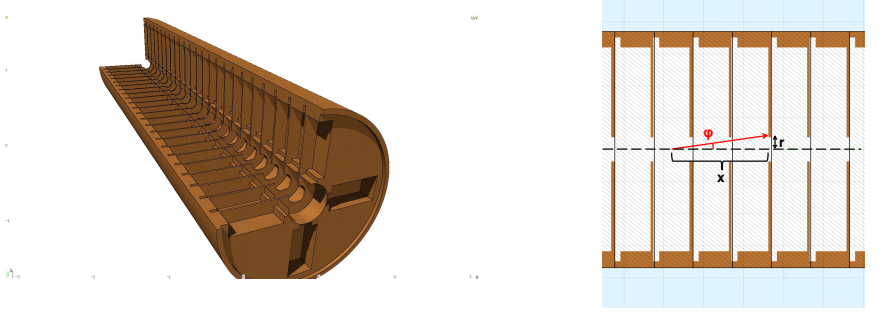

(a) The simulated geometry (b) Estimation of interaction angles of primaries

Fig. 6. Simulation of electron interactions with the CLIC accelerating structure

though the cavity. Hence, electrons emitted at different positions will have different energies when they reach the impact point. Since each cell has a thickness of approximately 1 cm, the maximum energy that an electron can gain in the RF cavity until it reaches cell 20 is approximately 20 MeV. Here it is assumed that the initial electron position is located in the radial center of the accelerating structure, as presented in 6(b). Therefore, the radial distance between the electron starting point and the loss position on the iris of the twentieth cell equals the iris radius (r = 0.375 cm). With x the longitudinal distance between the starting and the interaction position, the respective collision angles for different initial positions were calculated as:

$$\phi = \arctan \frac{r}{x} \tag{6}$$

The results of the simulation are summarised in Figure 7, where the differential fluence of electrons in the optical fibre, for different energies of primaries, is presented. The fluence refers to the total area of the optical fibre, and the set energy cut for the electrons crossing the fibre is 200 keV. Consequently, only the particles with an adequate energy for Cherenkov photon production are considered. The distributions show a large peak at energies slightly lower than the ones of the primaries, and a tail at lower energies. The high peaks can be created from the primaries entering the fibre, after losing an amount of energy due to bremsstrahlung while passing through the accelerating structure. Finally, it is demonstrated that when interacting with the cavity walls, primaries with an energy as low as 4 MeV will initiate electron showers that can cross the BLM.

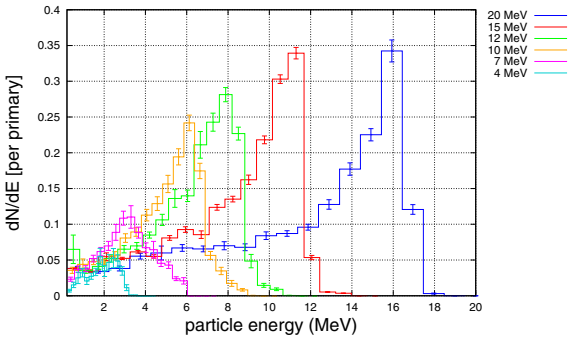

Fig. 7. Fluence of electrons with energies greater than 200 keV in an optical fibre, per primary in the CLIC accelerating structure

5. Conclusions

Electron field emission and RF breakdown are known phenomena in high gradient accelerating structures. Electrons emitted are accelerated in the RF field and impact on the cavity walls generating particle showers. From the data acquired at CTF3 and the FLUKA simulations performed, it has been shown that these electrons may cross the cavity walls and can be detected by BLMs. For the CLIC case, input powers of 60 MW can produce a signal of 410 μC in the optical fibre based BLMs, indicating a very high electron background around the accelerating structure. This will reduce the sensitivity of neighbouring BLMs, interrupting the detection of very low beam losses. Simulations of the particle fluence around the cavity can be a valuable tool for the detector position choice. Furthermore, the detector characteristics have to be taken into account in order to conclude on the type of BLM to be used. Nonetheless, the sensitivity of optical fibre BLMs to RF cavity induced signals renders them good candidates for accelerating stucture diagnostics, since they provide information on the RF pulse, the dark current lost in the structure and the occcurence of an RF breakdown without intervening the beam line. Such a tool can be highly useful in experiments like CTF3, where RF structures are located and examined in different beam lines.

References

[1] CLIC CDR, 2012. “A Multi-TeV linear collider based on CLIC technology: CLIC Conceptual Design Report”, edited by Aicheler, M., Burrows, P., Draper, M., Garvey, T., Lebrun, P., Peach, K., Phinney, N., Schmickler, H., Schulte, D., and Toge, N. (2012) CERN-2012-007

[2] Grudiev, A., 2010. “RF design and parameters of 12 GHz TD24_vg1.8_disk ”. The CERN EDMS (2010), edms.cern.ch/file/1070498/1/

[3] Bienvenu, G., Fernandes, P., Parodi, R., 1992. “An investigation on the field emitted electrons in travelling wave accelerating structures”. Nuclear Instruments and Methods in Physics Research A320 (1992) 1-8

[4] Palaia, A., Farabolini, W., Jacewicz, M., Ruber, R., Ziemann, V., 2013. Effects of RF breakdown on the beam in the Compact Linear Collider prototype accelerator structure. Phys. Rev. ST Accel. Beams 16, 081004

[5] K. Y. Ng , 2006. “Physics of Intensity Dependent Beam Instabilities”. World Scientific, Singapore (2006)

[6] Zenarro, R., Grudiev, A., Riddone, G., Wuensch, W., Tantawi, S., Wang, J. W., Higo, T., 2008. “Design and fabrication of CLIC test structures”. Conf. Proc: Linac08, Victoria, BC, Canada

[7] Navarro Quirante, J. L., Corsini, R., Degiovanni, A., Doebert, S., Grudiev, McMonagle, G., Rey, S., Syratchev, I., Tecker, F., Timeo, L., Wuensch, W., Kononenko, O., Solodko, A., Tagg, J., Wooley, B., Wu, X. W., 2014. “Effect of beam-loading on the breakdown rate of high gradient accelerating structures”. Conf. Proc: Linac2014, Geneva, Switzerland

[8] Thorlabs Inc., http://www.thorlabs.com/

[9] Hamamatsu Photonics K. K., http://www.hamamatsu.com/

[10] Texas Instruments Inc., http://www.ti.com/

[11] Jelley, J. V., 1958. “Čerenkov Radiation and its Applications”. Pergamon Press, London

[12] Van Hoorne, J. W., 2012. “Cherenkov Fibers for Beam Loss Monitoring at the CLIC Two Beam Module”. Masters thesis, Technische Universität Wien.

[13] Fowler, R. H. and Nordheim, L., 1928. “ Electron Emission in Intense Electric Fields”. Proceedings of the Royal Society of London, vol. 119, no 781, 1er mai 1928, p. 173181

[14] Ferrari, A., Sala, P. R., Fassò, A., and Ranft, J., 2005. “FLUKA: a multi-particle transport code”. CERN-2005-10 (2005), INFN/TC_05/11, SLAC-R-773

[15] Böhlen, T. T., Cerutti, F., Chin, M. P. W., Fassò, A., Ferrari, A., Ortega, P. G., Mairani, A., Sala, P. R., Smirnov, G., and Vlachoudis, V., 2014. “The FLUKA Code: Developments and Challenges for High Energy and Medical Applications”. Nuclear Data Sheets 120, 211-214 (2014)

[16] Grudiev, A., Wuensch, W., 2010. “Design of the main CLIC accelerating structure for CLIC Conceptual Design Report”. Conf. Proc: Linac2010, Tsukuba, Japan